

UNCLASSIFIED ~~CONFIDENTIAL~~

Copy 6  
RM L54D09a

NACA RM L54D09a



# RESEARCH MEMORANDUM

EFFECTS OF FENCES, LEADING-EDGE  
CHORD-EXTENSIONS, BOUNDARY-LAYER RAMPS, AND TRAILING-EDGE  
FLAPS ON THE LONGITUDINAL STABILITY OF A TWISTED AND-  
CAMBERED 60° SWEEPBACK-WING—INDENTED-BODY  
CONFIGURATION AT TRANSONIC SPEEDS

By Thomas L. Fischetti  
CLASSIFICATION CHANGED

Langley Aeronautical Laboratory  
Langley Field, Va.

To UNCLASSIFIED

**LIBRARY COPY**

JUN 17 1954

By authority of *Nasa TPA 8* Date *7-22-59*

*NB 9-14-59*

CLASSIFIED DOCUMENT

LANGLEY AERONAUTICAL LABORATORY  
LIBRARY, NACA  
LANGLEY FIELD, VIRGINIA

This material contains information affecting the National Defense of the United States within the meaning of the espionage laws, Title 18, U.S.C., Secs. 793 and 794, the transmission or revelation of which in any manner to an unauthorized person is prohibited by law.

## NATIONAL ADVISORY COMMITTEE FOR AERONAUTICS

WASHINGTON

June 17, 1954

~~CONFIDENTIAL~~

UNCLASSIFIED

~~CONFIDENTIAL~~

## NATIONAL ADVISORY COMMITTEE FOR AERONAUTICS

## RESEARCH MEMORANDUM

EFFECTS OF FENCES, LEADING-EDGE  
CHORD-EXTENSIONS, BOUNDARY-LAYER RAMPS, AND TRAILING-EDGE  
FLAPS ON THE LONGITUDINAL STABILITY OF A TWISTED AND  
CAMBERED 60° SWEEPBACK-WING--INDENTED-BODY  
CONFIGURATION AT TRANSONIC SPEEDS

By Thomas L. Fischetti

## SUMMARY

Tests have been made to obtain the longitudinal stability characteristics of a twisted and cambered 60° sweptback-wing--indented-body configuration with and without fences, leading-edge chord-extensions, boundary-layer ramps, and trailing-edge flaps at Mach numbers generally from 0.6 to 1.14.

The variation of pitching moment with lift for the basic configuration was undesirable at lift coefficients from 0.2 to 0.5 and indicated a large unstable break at a lift coefficient of approximately 0.5 throughout the Mach number range. The addition of fences at 50 and 75 percent of the wing semispan extended the usable lift-coefficient range to approximately a lift coefficient of 0.6 over the Mach number range tested. Leading-edge chord-extensions had only small effects on the longitudinal stability. Boundary-layer ramps (which were tested only at a Mach number of 0.60) improved the stability at moderate lift coefficients but caused the large unstable break to occur earlier. Partial-span trailing-edge flaps (which were also tested at only 0.60 Mach number) delayed the large unstable break to a lift coefficient of 0.7 for the basic configuration and a lift coefficient of 0.8 for the configurations with fences and leading-edge chord-extensions.

## INTRODUCTION

Exceptionally high lift-drag ratios have been obtained at transonic speeds for a moderately high aspect ratio twisted and cambered

~~CONFIDENTIAL~~

UNCLASSIFIED

60° sweptback-wing—indented-body configuration (ref. 1). However, configurations with wings of large sweep and moderate or high aspect ratios generally have poor longitudinal stability characteristics. For example, reference 2 shows that, for a wing-body configuration having a wing of approximately the same sweep and plan form as the wing of reference 1, the variations of pitching moment with lift at low speeds were undesirable at moderate lifts and indicated a large unstable break at a lift coefficient of about 0.75. Before practical use can be made of the configuration described in reference 1, it will be necessary to improve these characteristics.

References 2 and 3 showed that appreciable improvement in the moderate lift-coefficient range could be obtained with fences and that trailing-edge flaps delayed the large unstable break in the moment curve. Other low-speed investigations (refs. 4 and 5) of highly swept wings, which were not twisted and cambered, have indicated the effectiveness of leading-edge chord-extensions in delaying the unstable break in the moment curve.

Fences, leading-edge chord-extensions, boundary-layer ramps, and trailing-edge flaps have been tested on the same wing—indented-body configuration used in reference 1. The data reported herein were obtained over a Mach number range from 0.60 to 1.14 and an angle-of-attack range which generally varied from 1° to 17° for the basic configuration and the configurations with fences and leading-edge chord-extensions. For the configurations with either boundary-layer ramps or trailing-edge flaps, the Mach number range was limited to 0.60. The Reynolds number based on the mean aerodynamic chord varied from  $2.2 \times 10^6$  to  $2.8 \times 10^6$ .

## APPARATUS AND METHODS

### Tunnels

The aerodynamic characteristics in pitch of the basic configuration were obtained in the Langley 8-foot transonic pressure tunnel. The remainder of the tests were conducted at a later date in the Langley 8-foot transonic tunnel. Both facilities are single-return tunnels having slotted test sections which allow testing through the speed of sound without the usual effects of choking and blockage. The tests were conducted at atmospheric stagnation pressures.

### Configurations

The basic wing-body configuration used in these tests had a wing with  $60^\circ$  sweep of the quarter chord, an aspect ratio of 4, and a taper ratio of 0.333. The wing was twisted and cambered to approximate a uniform load at a lift coefficient of 0.25 and a Mach number of 1.4. The wing had 64A-series airfoil sections with a thickness distribution which varied from 12 percent at the root to 6 percent at 50 percent of the semispan and then remained constant at 6 percent to the tip (fig. 1). The body was indented for a Mach number of 1.4 according to a supersonic area rule. This concept, along with more details of the wing and the coordinates for the wing and body, has been presented in reference 1. A photograph of the basic configuration in the Langley 8-foot transonic pressure tunnel is shown in figure 2. A drawing of the basic configuration is presented in figure 3.

Fences were located at 50 and 75 percent of the wing semispan on both wing panels and were contoured to follow an approximation of the stream flow over the wing at the design condition. The fences extended slightly beyond the leading and trailing edges of the wing and had a constant height of 6 percent of the chord above the wing surface except for portions of the leading and trailing edges. Details of the fences are given in figure 3.

The leading-edge chord-extension configuration was composed of two chord-extensions having their inboard locations at 55 and 80 percent of the wing semispan on both wing panels. The extensions were formed by extending the mean camber line 15 percent of the local chord forward of the wing leading edge at the inboard locations and then tapering in plan form to zero extension at 80 and 100 percent of the wing semispan. The chord-extensions had the same thickness distribution as the basic wing except in the region from the wing leading edge to the wing maximum thickness where the thickness distribution was modified slightly to provide a smooth fairing (fig. 3).

Consideration of the flow over a highly swept wing has led to the design of a boundary-layer ramp as shown in figure 3. The purpose of this ramp is to force the low energy air in the boundary layer off the wing surface in order to allow it to mix with the higher energy air in the stream. It is believed that this mixing would be conducive to improved flow over the remainder of the wing surface. In this manner, the action of the ramps is similar to that of vortex generators (ref. 3). However, the effect of the mixing action of the ramps would be felt over the entire chord rather than over a small portion of the chord as is the case with vortex generators. As investigated, the ramps were wedge shaped in cross section and were located at each 10 percent of the span from 40 percent of the wing semispan to the tip on both wing panels. The ramps extended

from leading edge to trailing edge and the vertical face was contoured to the calculated stream flow over the wing in the same manner as for the fences.

The trailing-edge flaps had chords of 0.20 of the wing chord and were located with their hinge lines coincident with the wing trailing edge. The flaps extended from approximately 11 percent to 41 percent of the wing semispan on both wing panels and were deflected  $45^\circ$  as measured from the lower surface of the wing trailing edge in a plane perpendicular to the wing trailing edge (fig. 3).

### Tests

The model was attached to a sting support system by means of an electrical strain-gage balance. Lift, drag, and pitching-moment coefficients have been determined about a point on the body axis being at the same longitudinal position as the quarter-chord point of the mean aerodynamic chord. For the basic configuration and the configurations with fences and leading-edge chord-extensions, tests were conducted over a Mach number range which varied from 0.60 to 1.14. For the configuration with boundary-layer ramps and for the trailing-edge flaps in combination with either the basic configuration or the configurations with fences and leading-edge chord-extensions, the tests were limited to a Mach number of 0.60. The angle of attack was measured by a pendulum-type inclinometer and generally varied from  $1^\circ$  to  $17^\circ$  but in some cases was as high as  $19^\circ$ . The Reynolds number based on a mean aerodynamic chord of 6.5 inches varied from  $2.2 \times 10^6$  to  $2.8 \times 10^6$ .

### Accuracy

The accuracy of the measured lift and pitching-moment coefficients based on balance design was  $\pm 0.002$  and  $\pm 0.003$ , respectively. Because of difficulties with the electrical strain-gage balance, the accuracy of the drag data was believed to be impaired and therefore is not presented. The accuracy of the measured angle of attack is believed to be better than  $\pm 0.15^\circ$ . Unpublished results have indicated that the local deviations from the average free-stream Mach number in the region of the model in the Langley 8-foot transonic pressure tunnel for the Mach numbers of this investigation are essentially no higher than those reported for the Langley 8-foot transonic tunnel in reference 6 in which the deviation at subsonic Mach numbers was 0.003 with an increase to 0.010 at a Mach number of 1.13. The data presented are essentially free of boundary-reflected disturbances.

## RESULTS AND DISCUSSION

## Basic Configuration

The variation of pitching-moment coefficient with lift coefficient for the basic configuration and the configurations with fences and chord-extensions for the various test Mach numbers is presented in figure 4(a). The free-stream Mach number is designated in the figures by the letter M. For the basic configuration, nonlinearities occurred in the lift-coefficient range of approximately 0.2 to 0.5 over the entire Mach number range. Increasing the Mach number reduced the abruptness of the nonlinearities and at the higher Mach numbers delayed them to slightly higher lift coefficients. These nonlinearities are indicative of large movements of the aerodynamic-center location. Because of these nonlinearities, there is a forward movement of the aerodynamic center of approximately 24 percent of the mean aerodynamic chord at a Mach number of 0.60 and lift-coefficient range of 0 to 0.35. With an increase to a lift coefficient of about 0.45, there is an approximately equal movement rearward. For a lift coefficient above 0.5, the moment curve shows that there is another unstable break which is of a large magnitude. This large unstable break occurred at approximately the same lift coefficient throughout the Mach number range.

It will be noted that the variation of angle of attack with lift coefficient (fig. 4(b)) for Mach numbers of 0.60 to 1.03 shows a nonlinearity in the regions of instability indicated in figure 4(a). For a Mach number of 0.60, this nonlinearity amounts to a decrease in lift-curve slope in the unstable region of approximately 0.20 to 0.35 lift coefficient and an increase in the stable region of 0.35 to 0.50 (figs. 4(a) and (b)). Figure 4(b) also indicates that a large decrease in lift-curve slope occurs above the lift coefficient corresponding to the large unstable break in the moment curve.

The similarity of the variations in pitching moment with lift for the basic configuration of this test and the configuration of reference 2 which was tested at low speeds is an indication of the existence of a similar flow phenomenon over both wings. The pressure distributions over the wing reported in reference 2 showed that the nonlinearities in the pitching-moment characteristics at moderate lift coefficients are due to a decrease in lift-curve slope at the outboard sections and the subsequent increase in lift-curve slope on the sections inboard of the tip. Similarly, the early instabilities noted in figure 4(a) are due to the decrease in lift-curve slope and the stable tendencies at the higher lift coefficients are due to the subsequent increase in lift-curve slope. It is believed that the decrease in lift-curve slope over the outboard sections is associated with the start of outflow of the boundary layer

in the wing-trailing-edge region. The subsequent increases of lift-curve slope are associated with the buildup of a leading-edge separation vortex. Reference 2 shows that the large unstable break in the pitching moment occurred when flow separation at the wing tip spread inboard. For a 6-percent-thick  $45^\circ$  sweptback wing, reference 7 showed that a leading-edge separation vortex has a predominant influence on the upper-surface flow at Mach numbers up to 0.80 and that at higher Mach numbers shocks have a predominant influence on the flow. Since the configuration of the present investigation has a wing with  $60^\circ$  of sweep and a body which has been indented to reduce the intensity of shock disturbances, the Mach number at which shocks become important is probably higher than shown in reference 7 and may be near a Mach number of 1.0. Thus, the low-speed results of reference 2 are probably applicable up to Mach numbers somewhat less than 1.0.

#### Effect of Fences

The addition of fences at 50 and 75 percent of the wing semispan resulted in an improvement in the instability at moderate lift coefficients and a delay in the large unstable break (fig. 4(a)). The over-all effect of the addition of fences was that the usable lift range for this configuration was increased to a lift coefficient of approximately 0.60 from a Mach number of 0.60 to 1.14. The effectiveness of the fences is shown in reference 2 to be directly attributable to their ability to allow the tip sections to maintain lift to high angles of attack. Figure 4(b) shows that adding the fences resulted in a decrease in the nonlinearity of the lift curves at moderate lift coefficients and in an increase in lift coefficient at high angles, as would be expected.

#### Effect of Leading-Edge Chord-Extensions

Adding either 15-percent chord-extensions at 55 and 80 percent of the wing semispan or a single 10-percent chord-extension, which had its inboard location at 65 percent of the wing semispan and which tapered to zero extension at 100 percent of the wing semispan (data not presented), produced only small effects in the moment curves (fig. 4(a)). Both references 4 and 5 have shown that leading-edge chord-extensions can be used to improve the stability characteristics of wings having high degrees of sweep. However, both of these investigations were conducted on lower-aspect-ratio wings than the wing of the present investigation. It is believed that the chord-extensions were less effective on the wing of this investigation because of its higher aspect ratio.

### Effect of Boundary-Layer Ramps

Boundary-layer ramps improved the stability at moderate lift coefficients (fig. 5). However, at higher lift coefficients, the ramps caused the large unstable break in the moment curve to occur 0.1 lift coefficient earlier than for the basic configuration.

### Effect of Trailing-Edge Flaps

The effect of partial-span trailing-edge flaps at a Mach number of 0.60 was primarily a delay of the large unstable break to a lift coefficient of 0.70 for the basic configuration and to a lift coefficient of 0.80 for the configurations with fences and leading-edge chord-extensions (fig. 6(a)). Figure 6(b) shows that the trailing-edge flaps increased the linearity of the lift curves for these configurations.

The devices investigated in these tests have provided some improvement in the stability of this  $60^\circ$  swept-wing—indented-body configuration at moderate lift coefficients. However, the large unstable break at stall still remains a serious stability problem. It is believed that further improvements in stability may be realized by the use of either spanwise slots near the wing trailing edge or by a favorable location of a tail surface.

### CONCLUSIONS

Results of an investigation at transonic speeds of the longitudinal stability characteristics of a twisted and cambered  $60^\circ$  sweptback-wing—indented-body configuration with and without various devices added to the wing for improvement of stability indicate the following remarks:

1. For the basic configuration, the variation of pitching moment with lift showed that there were nonlinearities in the lift-coefficient range of approximately 0.2 to 0.5 and a large unstable break in the moment curve at a lift coefficient of approximately 0.5 over the Mach number range of 0.60 to 1.14.
2. Fences located at 50 and 75 percent of the wing semispan extended the usable lift-coefficient range to approximately 0.60 over the Mach number range of 0.60 to 1.14.
3. The leading-edge chord-extensions tested had only small effects on the longitudinal stability.



4. Boundary-layer ramps (at a Mach number of 0.60) improved the stability at moderate lift coefficients but caused the large unstable break to occur 0.1 lift coefficient earlier than the basic configuration.

5. Partial-span trailing-edge flaps at a Mach number of 0.60 delayed the large unstable break to a lift coefficient of 0.7 for the basic configuration and to a lift coefficient of 0.8 for the configurations with fences and leading-edge chord-extensions.

Langley Aeronautical Laboratory,  
National Advisory Committee for Aeronautics,  
Langley Field, Va., March 24, 1954.

## REFERENCES

1. Whitcomb, Richard T., and Fischetti, Thomas L.: Development of a Supersonic Area Rule and an Application to the Design of a Wing-Body Combination Having High Lift-to-Drag Ratios. NACA RM L53H31a, 1953.
2. Weiberg, James A., and Carel, Hubert C.: Wind-Tunnel Investigation at Low Speed of a Wing Swept Back  $63^\circ$  and Twisted and Cambered for a Uniform Load at a Lift Coefficient of 0.5. NACA RM A50A23, 1950.
3. Weiberg, James A., and McCullough, George B.: Wind-Tunnel Investigation at Low Speed of a Twisted and Cambered Wing Swept Back  $63^\circ$  With Vortex Generators and Fences. NACA RM A52A17, 1952.
4. Lowry, John G., and Schneider, Leslie E.: Investigation at Low Speed of the Longitudinal Stability Characteristics of a  $60^\circ$  Swept-Back Tapered Low-Drag Wing. NACA TN 1284, 1947.
5. Furlong, G. Chester: Exploratory Investigation of Leading-Edge Chord-Extensions To Improve the Longitudinal Stability Characteristics of Two  $52^\circ$  Sweptback Wings. NACA RM L50A30, 1950.
6. Ritchie, Virgil S., and Pearson, Albin O.: Calibration of the Slotted Test Section of the Langley 8-Foot Transonic Tunnel and Preliminary Experimental Investigation of Boundary-Reflected Disturbances. NACA RM L51K14, 1952.
7. West, F. E., Jr., and Henderson, James H.: Relationship of Flow Over a  $45^\circ$  Sweptback Wing With and Without Leading-Edge Chord-Extensions to Longitudinal Stability Characteristics at Mach Numbers From 0.60 to 1.03. NACA RM L53H18b, 1953.

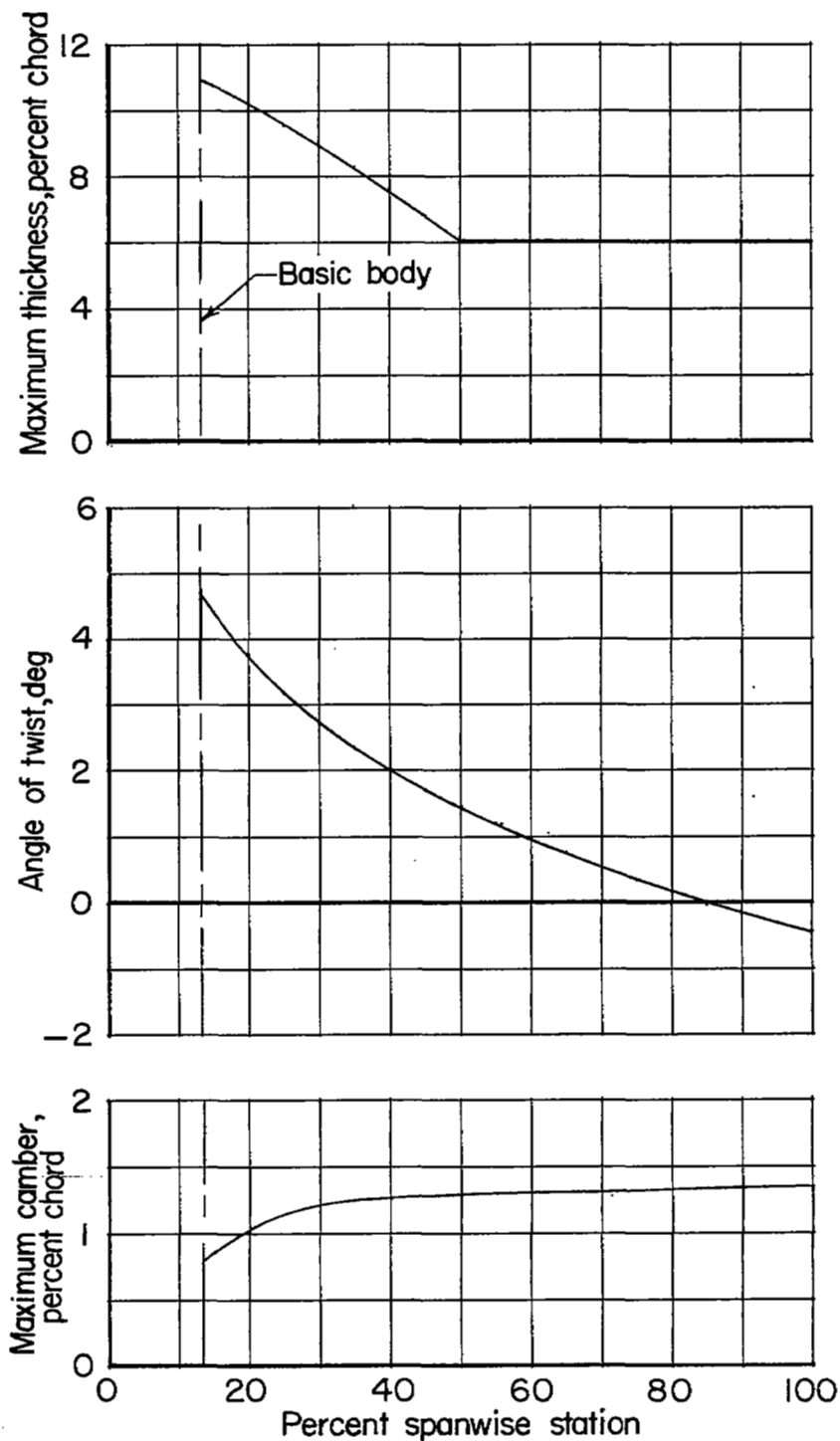
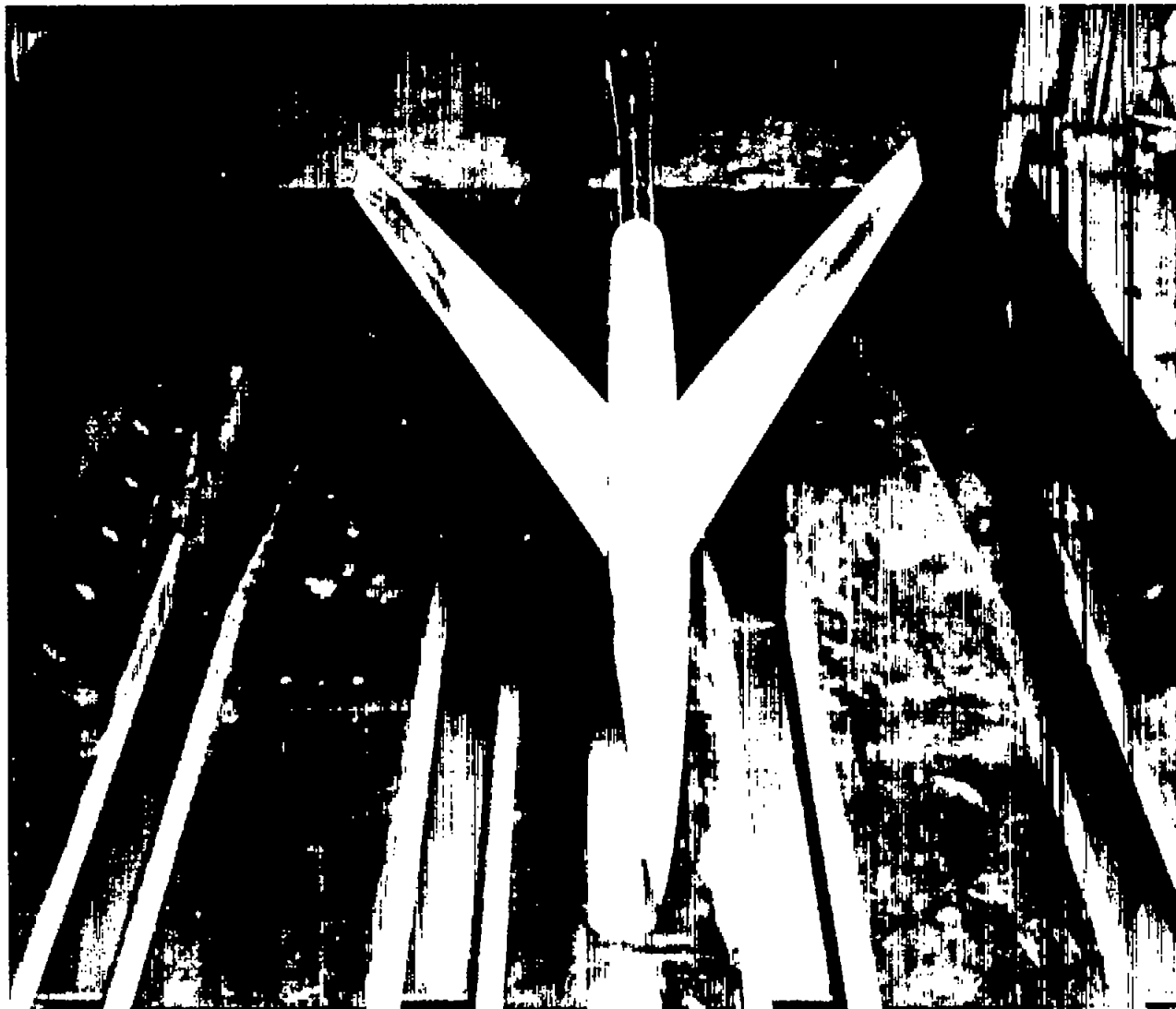


Figure 1.- Spanwise distributions of section thickness ratio, angle of twist, and maximum camber for the basic wing-body configuration.



L-82137.1

Figure 2.- Basic model in the Langley 8-foot transonic pressure tunnel.

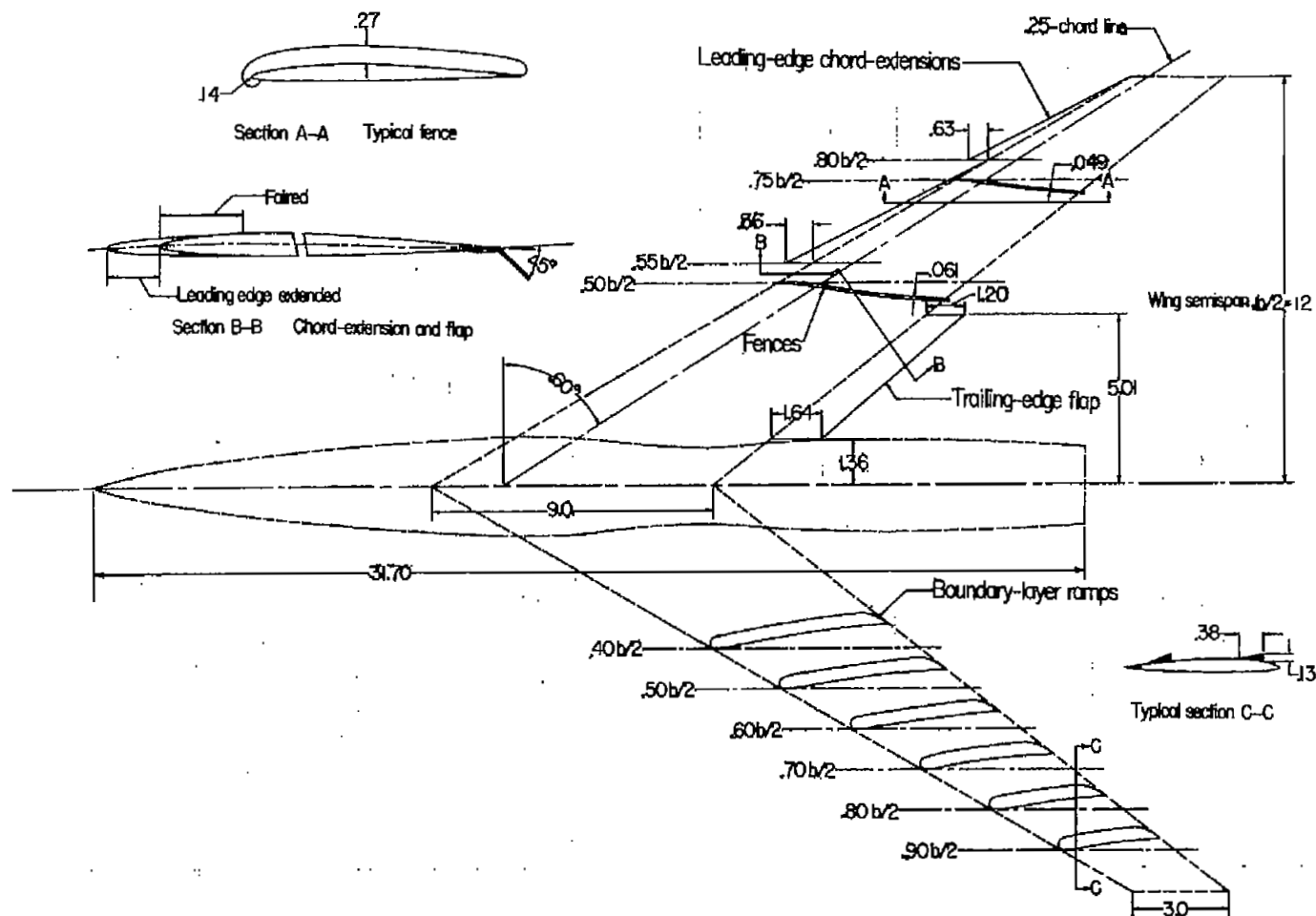
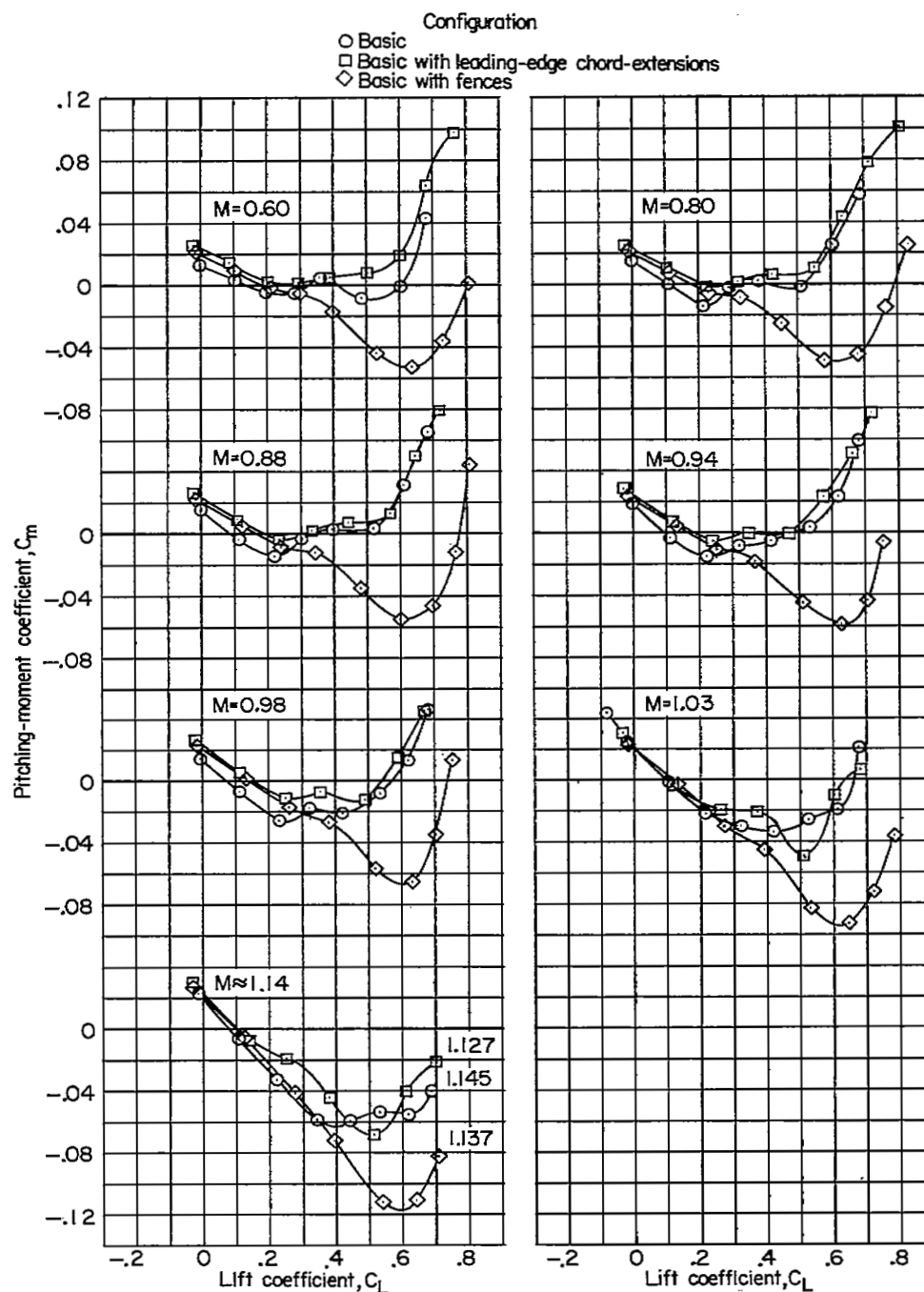
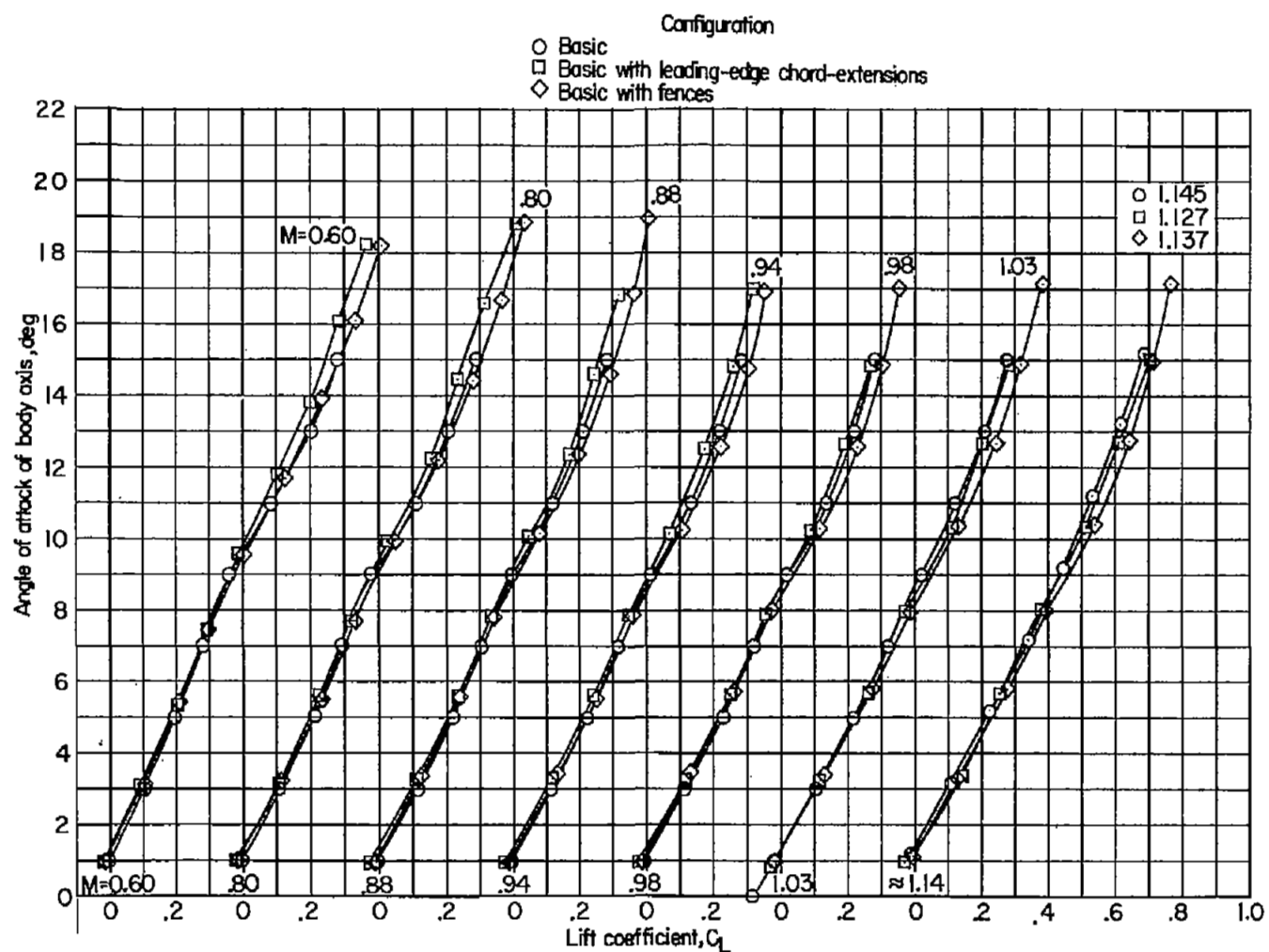


Figure 3.- Details of model with fences, leading-edge chord-extensions, boundary-layer ramps, and trailing-edge flaps. Fences, leading-edge chord-extensions, and trailing-edge flaps shown on right wing panel; boundary-layer ramps shown on left wing panel. All dimensions are in inches unless otherwise specified.



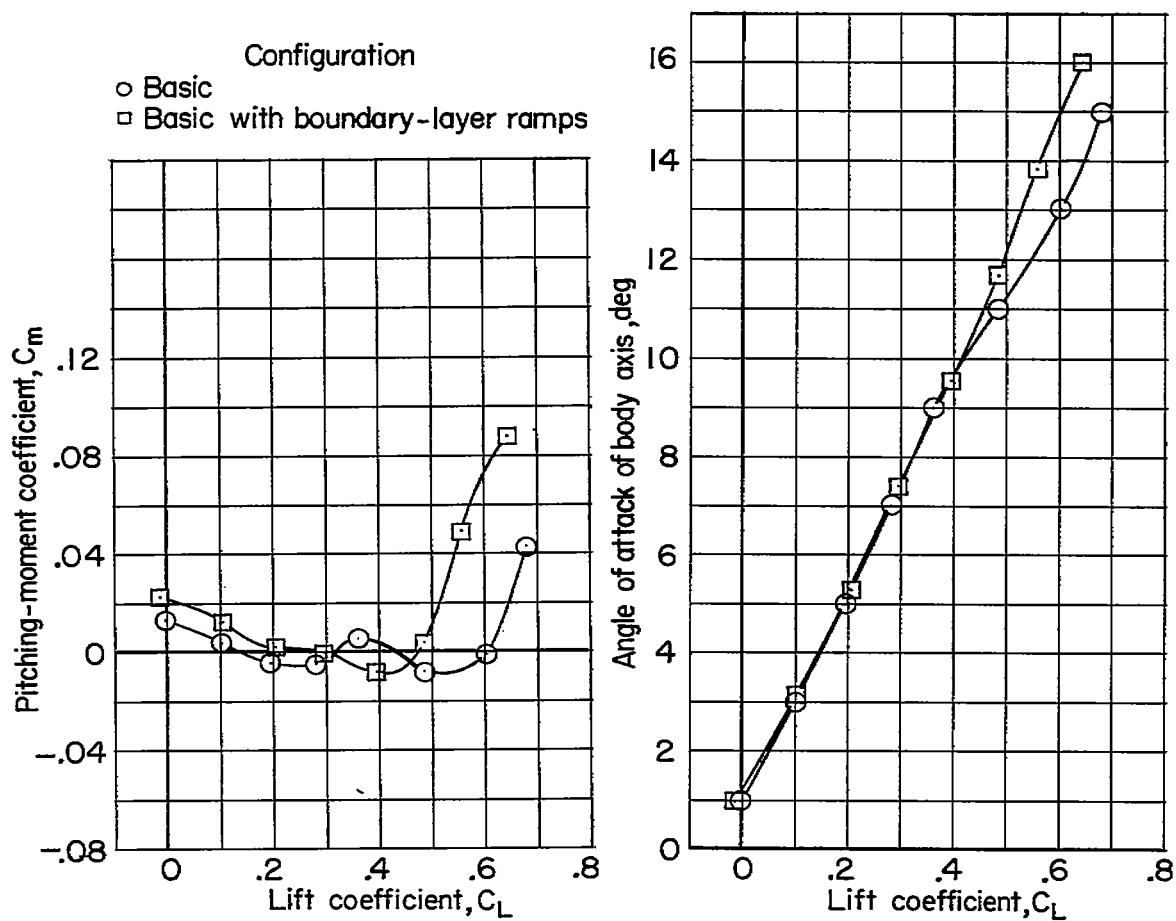
(a) Pitching-moment coefficient.

Figure 4.- Variation of pitching-moment coefficient and angle of attack with lift coefficient for the basic configuration and the configurations with fences and leading-edge chord-extensions.



(b) Angle of attack of body axis.

Figure 4.- Concluded.

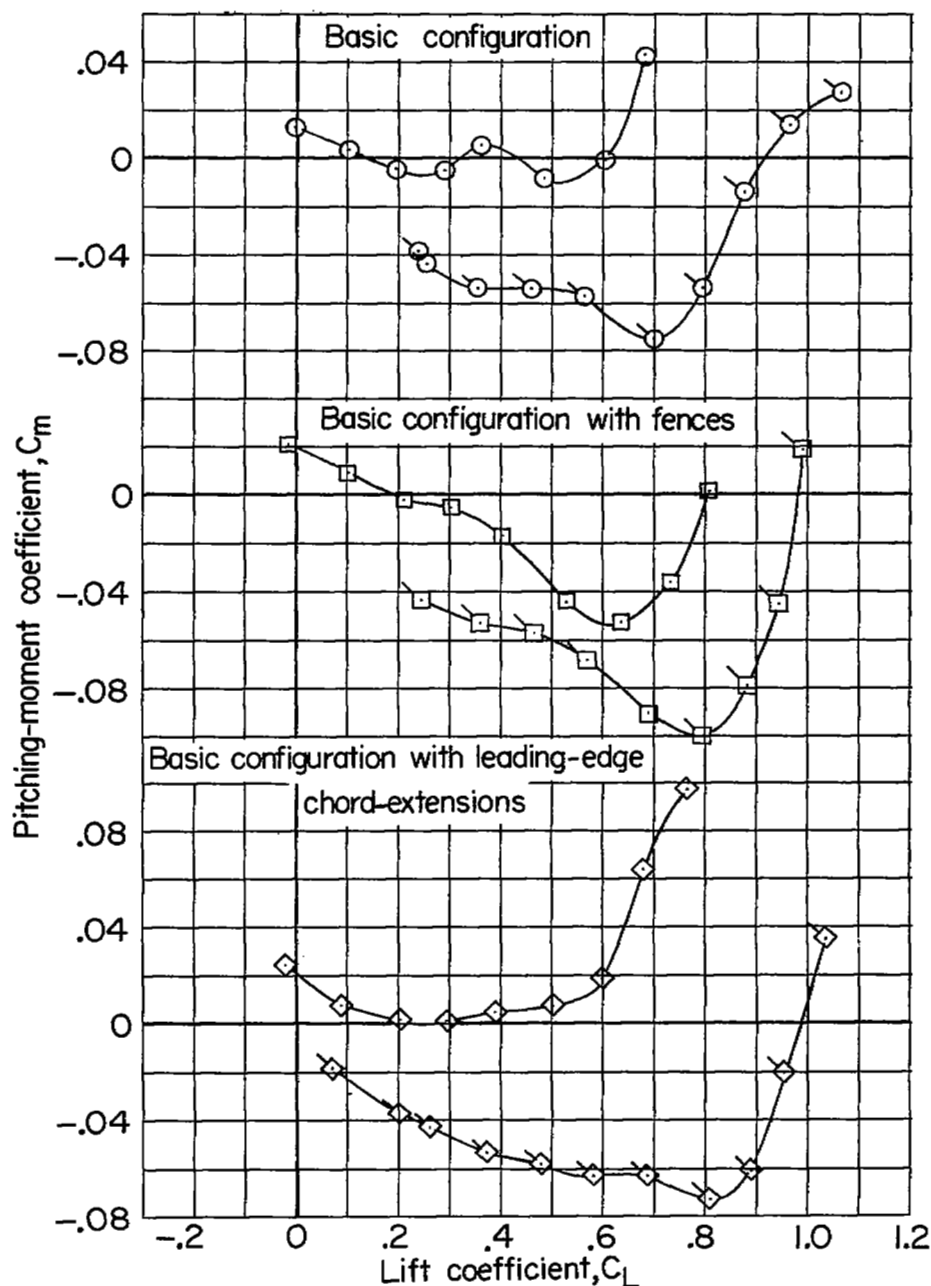


(a) Pitching-moment coefficient.

(b) Angle of attack of body axis.

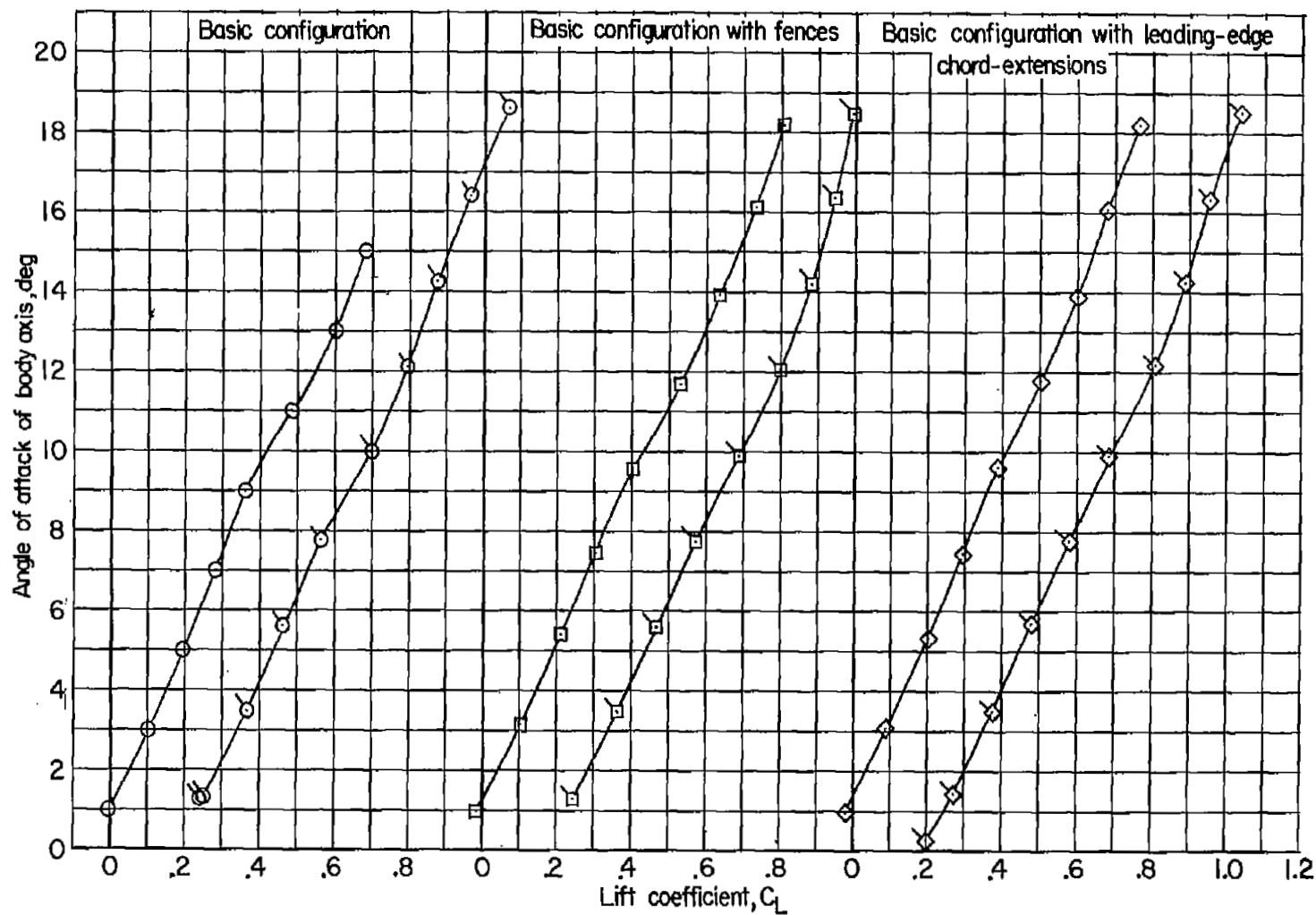
Figure 5.- Variation of pitching-moment coefficient and angle of attack with lift coefficient for the configuration with boundary-layer ramps.  $M = 0.60$ .





(a) Pitching-moment coefficient.

Figure 6.- Variation of pitching-moment coefficient and angle of attack with lift coefficient for the basic configuration and the configurations with fences and leading-edge chord-extensions in combination with a partial-span trailing-edge flap.  $M = 0.60$ . (Flagged symbols indicate configuration with flaps deflected  $45^\circ$ .)



(b) Angle of attack of body axis.

Figure 6.- Concluded.

[REDACTED]



[REDACTED]

[REDACTED]

[REDACTED]

[REDACTED]

[REDACTED]